Wallis, D. J., Wright, P. J., Soley, D. E. J., Koker, L., Uren, M. J., & Martin, T. (2012). 2 dimensional electron gas uniformity of GaN HFET layers on SiC. Journal of Crystal Growth, 338(1), 125-128. 10.1016/j.jcrysgro.2011.10.054

Link to published version (if available):
10.1016/j.jcrysgro.2011.10.054

Link to publication record in Explore Bristol Research
PDF-document

2 Dimensional Electron Gas Uniformity of GaN HFET Layers on SiC

DJ Wallis[a], PJ Wright, DEJ Soley, L Koker, MJ Uren[b] and T Martin[c]

QinetiQ, Malvern Technology Centre, St Andrews Road Malvern, WR14 3PS, UK.

[a] Present address: Department of Materials Science and Metallurgy, University of Cambridge, Pembroke Street, Cambridge, CB2 3QZ, United Kingdom.

[b] Present address: University of Bristol, School of Physics, HH Wills Physics, Laboratory, Tyndall Avenue, Bristol, BS8 1TL

[c]Present address: IQE Plc, St Mellons, Cardiff

Abstract

As GaN power transistor technology matures it is increasingly important to understand any links between substrate “quality”, epi-layer growth and electrical characteristics of the 2-dimensional electron gas (2DEG) which forms the active part of devices. We present a study which makes use of full wafer mapping techniques to examine these relationships. Substrate off-cut is shown to be an important parameter in controlling the uniformity of GaN HFET device layers on SiC substrates.

Key Words
A1 Characterisation
A3 Metal Organic Vapour Phase Epitaxy
B1 Nitrides
B2 Semiconducting III-V Materials
B3 Field Effect Transistors

1 Introduction

AlGaN/GaN based microwave hetero-junction field-effect transistors (HFETs) have the potential to give dramatic improvements in power applications compared to existing GaAs devices. Such devices have been demonstrated by many groups with radio frequency (rf) power densities of 5W/mm and above [1]. Over the last few years the maturity of GaN HFET technology has increased and commercial devices are now available from several US and Japanese suppliers [2,3,4,5]. A significant amount of research effort is therefore now being concentrated on the refinement of the AlGaN/GaN growth process in order to deliver consistent material properties for the production of transistor devices to well defined specification.

Due to the lack of large area single crystal GaN substrates and the thermal requirements of devices with high power densities, the substrate of choice for the growth of high power GaN devices is semi-insulating SiC. As a result of the 3.5% lattice mismatch at the SiC/GaN hetero-epitaxial interface, a high threading dislocation density of around 10^9 to 10^{10} cm^{-2} is reported in most HFET devices [6]. Despite these high defect densities, devices with high performance and reliability have been produced. However, due to the relative immaturity and technical challenges of growing semi-insulating SiC compared to other common semiconductor substrates, in addition to threading dislocations, a significant quantity of defects may be present in the substrate which are transferred into the active parts of the device layer. For example, it is well known that micropipes, which represent large screw dislocations with open cores, are present in SiC substrates and are transferred into the GaN epi-layer during growth [7,8]. Other defects found in SiC substrates include graphite inclusions, grain boundaries and poly-type inclusions. One of the significant issues for a reliable GaN technology is a clear understanding of the link between substrate properties, GaN growth parameters and their influence on the final device performance and reliability. In this article we report results of a study of GaN HFETs grown on to 50mm SiC substrates which attempts to correlate substrate defects with properties of the 2-Dimensional Electron Gas (2DEG) which forms the active channel of HFET devices.

1.1 Experimental Details

The epi-layers studied were grown by MOCVD in a Thomas-Swan close coupled shower head reactor as described elsewhere [9]. The basic layer structure consists of a 1.9μm Fe doped GaN buffer layer and a 25nm AlGaN barrier layer with an Al fraction of approximately 0.25. Full wafer images shown in this article were collected using a proprietary full wafer imaging system which has been developed by the authors. This system allows optical imaging of complete wafers before and after growth with a lateral resolution of about 10μm and a height resolution of about 10nm. Since complete wafers are imaged on the same system before and after growth, tracking of individual defects from the substrate to the epi-layer is possible. Atomic Force Microscopy (AFM) data was collected on a Digital Instruments Nanoscope Dimension III AFM in tapping mode.

2. Results and Discussion

Figure 1a) shows a crossed polariser image of a 50mm diameter SiC substrate collected on the whole wafer imaging system. The contrast in this image is due to birefringence in the SiC caused by strain along the crystal c-axis [10]. This strain results in rotation of the polarised light as it is transmitted through the substrate and therefore provides a map of the strain fields around crystallographic defects such as micropipes and crystal tilt boundaries. For the particular substrate shown, it can be seen that the crystalline quality varies significantly across the wafer. To the right hand side of figure 1a) there is a high density of crystal defects with the left hand side of the image showing evidence of very few defects except at the extreme wafer edge. Figure 1b) shows a transmitted light image of the same wafer collected following epi-layer growth. (The slight vertical banding and darker crescent on the right of the figure are imaging artefacts). In this imaging mode, the GaN epi-layers acts as an etalon which results in constructive and destructive interference of the transmitted light as the thickness of the epi-layer changes. The image therefore provides a relative thickness map of the epi-layer. It can be seen from the brightness (colour) changes in figure 1b) that defects present in the substrate have an impact on the epi-layer growth and induce local changes in the growth rate and therefore total thickness of the epi-layer. The transition from dark to light (pink to green) in the image represents a change in thickness of about 30nm in the total film thickness of 1.9μm. By comparing Figures 1a) and b) individual features in the crossed polariser image of the substrate may be mapped directly onto the features seen after growth. Conventional wisdom, would predict that such defects and disruption to the growth would have a negative impact on the electrical properties of the 2DEG formed at the GaN/AlGaN interface. However, figure 1c) gives a map of sheet resistivity of the 2DEG measured using a Lehighton contactless resistivity mapper. This resistivity map is generated from a 55 point grid measured across the wafer with a 5mm edge exclusion zone. Interestingly, the regions of the wafer which show a large density of defects in figure 1a) and disturbed growth in figure 1b) have uniform sheet resistivity and are at the lower end of the spread in measured resistivity values. This indicates that the 2DEG is undisturbed by the strain fields imaged in the crossed polariser image. In contrast, an approximately 10% increase in sheet resistivity is seen to the left of figure 1c) which correlates with the region of the substrate which is relative free of defects in figure 1b).

Inspection of figure 1b) at higher resolution reveals a region of islanded contrast on the wafer which can be correlated with the region of high R_{sheet} in figure 1c). This islanded contrast is shown in figure 2a) which is an enlarged region from within the circled area of the wafer in figure 1b). In this enlarged image, the epi-layer has small localised height variations which AFM (figure 2b) confirms to be growth islands of about 30μm in diameter and about 30nm in height. These islands are present all over the circled area in figure 1b). Outside the area circled in figure 1b), the epi-layer is much smoother as shown in figure 3 which gives a similarly enlarged transmitted light image and AFM data from close to the centre of the wafer.

Features which have the appearance of scratches can also be seen in figures 2a) and 3a). These are consistently seen for our epi-layer growth on SiC and are believed to be due to sub-surface damage left during the SiC polishing process. As for the defects seen in the crossed polariser image shown in figure 1a), these disruptions to the crystallography cause small modifications to the local GaN growth rate, causing the scratches to be revealed in the transmitted light images after epi-layer growth. No evidence for an impact on the sheet resistivity of long individual scratches or clusters of scratches has been seen in Lehighton resistivity maps, although it should be noted that the resolution of the Lehighton instrument is several mm and therefore it can not be ruled out that these features do have an effect, but the instrument resolution is not sufficient to reveal them.

The origins of the islanded epi-layer morphology seen in figure 2 are revealed by high resolution AFM of the epi-layer surface. Figure 4) shows a series of AFM images collected from across the wafer surface. Figure 4a) was collected from the left hand side of the wafer shown in figure 1b) and shows the step terrace surface of the AlGaN barrier surface. The small pits that are observed in the AFM indicate the locations where threading dislocations appear at the epi-layer surface [11]. The step terrace structure of this image shows a random step direction with relatively large terraces. This is consistent with growth on a very close to on-axis crystal surface where the epi-layer grows via the formation of islands due to the limited surface diffusion length of add-atoms. The estimated off-cut of the wafer in this region, based on the terrace length and step height, is about 0.1 degrees. This is consistent with the facet angle for an island 30μm in diameter and 30nm high as seen in figure 3b).

Figures 4b) and c) show similar AFM images collected from the centre and the right hand side of the wafer outside the circled region. In both cases the steps and terraces seen in the AFM are approximately vertically aligned and are consistent with growth on an off-cut crystal surface where growth proceeds by a step flow mechanism. The off-cut estimated from the terrace lengths and step heights measured from figures 4b and c are 0.21 degrees and 0.25 degrees respectively. These results suggest that the off-cut across the wafer is increasing from left to right. X-ray diffraction measurements (not shown) performed on this and other SiC substrates in this batch also confirm that the SiC crystal planes bend across such wafers by up to 1.0 degrees. However, bow measurements of the optical surface of the wafer suggest that the value of wafer bow is relatively low (6μm across the 50mm wafer diameter). Therefore these measurements are consistent with an increasing off-cut angle across the substrates as shown schematically in figure 5 due to bending of the SiC crystal planes. Thus the region of high sheet resistivity seen in figure 1c) may be correlated to the islanded growth mode of the GaN on a region of the substrate which is very close to on-axis.

Sheet resistance is related to two different fundamental properties of the 2DEG, i.e. the sheet carrier density, N_s, and the carrier mobility, μ, since $R_{sheet} = 1/N_s\mu e$ where, e, is the electron charge. Thus it is of interest to know which of these fundamental properties of the electron gas is affected by the change in growth mode. Spot Mercury Capacitance/Voltage (CV) measurements of carrier density on several wafers suggest that the increase in R_{sheet} for growth on close to on-axis regions of substrate are related to reductions in Ns and not changes in carrier mobility.

3. Conclusion

In conclusion, we have used full wafer mapping techniques to look at the correlation of SiC substrate features and the properties of the 2DEG in AlGaN/GaN

HFET structures. There is no direct evidence for an impact of crystallographic defects in the SiC affecting the 2DEG, although such defects do locally change the GaN growth giving rise to small changes in growth rate and could impact the reliability of devices. Instead, variations in substrate off-cut result in significant changes in the GaN growth mode. A transition from an island growth mode to a step flow growth mode for off-cuts above about 0.1 degrees is seen. This off-cut variation is also correlated with changes in the value of R_{sheet} across individual wafers and from wafer to wafer. Mercury CV measurements suggest that these changes in R_{sheet} arise from changes in the carrier density of the 2DEG. At present the origins of the change in carrier concentration across the wafer are not known. However it is noted that variations in the incorporation of Carbon impurities with substrate off-cut have been seen for GaAs during MOCVD growth [12]. As Carbon is a deep acceptor in GaN [13] a local increase in Carbon impurities could reduce the charge in the 2DEG. Clearly, accurate control of substrate off-cut and substrate crystal plane curvature are important parameters in order to achieve a repeatable growth process for the production of GaN based HFET devices.

Acknowledgement

This work was support by the UK MoD as part of the European Defence agency program, Korrigan. The authors wish to Acknowledge IQE Europe ltd for performing contactless “Lehighton” measurements.

References

[1]Y. F. Wu, A. Saxler, M. Moore, R. P. Smith, S. Sheppard, P. M. Chavarkar, T. Wisleder, U. K. Mishra, and P. Parikh, *IEEE Elec. Dev. Lett.* 25 (2004) 117-119.

[2] http://global-sei.com/tr/pdf/electronics/71-15.pdf (2011)

[3] http://www.cree.com/products/wireless.asp (2011)

[4] www.nitronex.com (2011)

[5] http://www.rfmd.com/foundry/default.aspx (2011)

[6] A.L. Corrion, C. Poblenz, F. Wu and J.S. Speck, Journal of Applied Physics, 103 (2008), 093529 - 093535

[7] H. Sazawa, T. Kato, K. Kojima, K. Furuta, K. Hirata, M. Kosaki, M. Kinoshita, T. Mitani, S. Nakashima and H. Okumura, Materials Science Forum, 556-557, (2007), 1043-1046

[8] L. Kirste S. Mu¨ller R. Kiefer , R. Quay, K. Ko¨hler, N. Herres, Applied Surface Science 253 (2006) 209–213

[9] R.S. Balmer, D.E.J. Soley, A.J. Simons, J.D. Mace, L. Koker, P.O. Jackson, D.J. Wallis, M.J. Uren and T. Martin, Phys. Stat. Sol. (c) 3 (2006), 1429-1434

[10] S.H. Park, M.J. Loboda, M.J. Spaulding, Materials Science Forum. 527-529, (2006), 721-724.

[11] R.A Oliver, M.J Kappers,, J Sumner, R Datta, C.J Humphreys, *Journal of Crystal Growth* 289 (2), (2006). 506-514

[12] GB Stringfellow, “Organometallic Vapour-Phase Epitaxy – Theory and Practice”, academic Press, (1999) p396-398

[13] J. L. Lyons, A. Janotti, and C. G. Van de Walle, Applied Physics Letters, **97**, (2010), 152108-152110

Figure Captions

Figure 1 (colour on line) a) Full wafer crossed polariser image of a 50mm SiC substrate before growth, b) full wafer transmitted light image of the same wafer after epi-layer growth of an HFET structure and c) Lehighton contactless sheet resistivity map of this epi-layer with a 5mm edge exclusion zone. The circled area in figure 1b) indicates a region of islanded morphology.

Figure 2 (colour on line) a) Enlarged transmitted light image taken from within the circled area of figure 1b) and b) typical 60μm square AFM image of the AlGaN surface in the circled area of figure 1b). The Z-range of figure 2b) is 30nm

Figure 3 (colour on line) a) Enlarged transmitted light image taken from outside the circled area of figure 1b) close to the centre of the wafer and b) typical 60μm square AFM image of the AlGaN surface outside the circled area of figure 1b). The Z-range of figure 3b) is 8nm.

Figure 4) (colour on line) 2μm square AFM images of the AlGaN surface taken from a) the left hand side of figure 1b), i.e. inside the circled area, b) the centre of figure 1b) and c) the right hand side of figure 1b). The Z-ranges of the images are 3nm, 5nm and 5nm respectively.

Figure 5) schematic diagram of crystal plane bending in the SiC substrate.

Figures

Figure 1

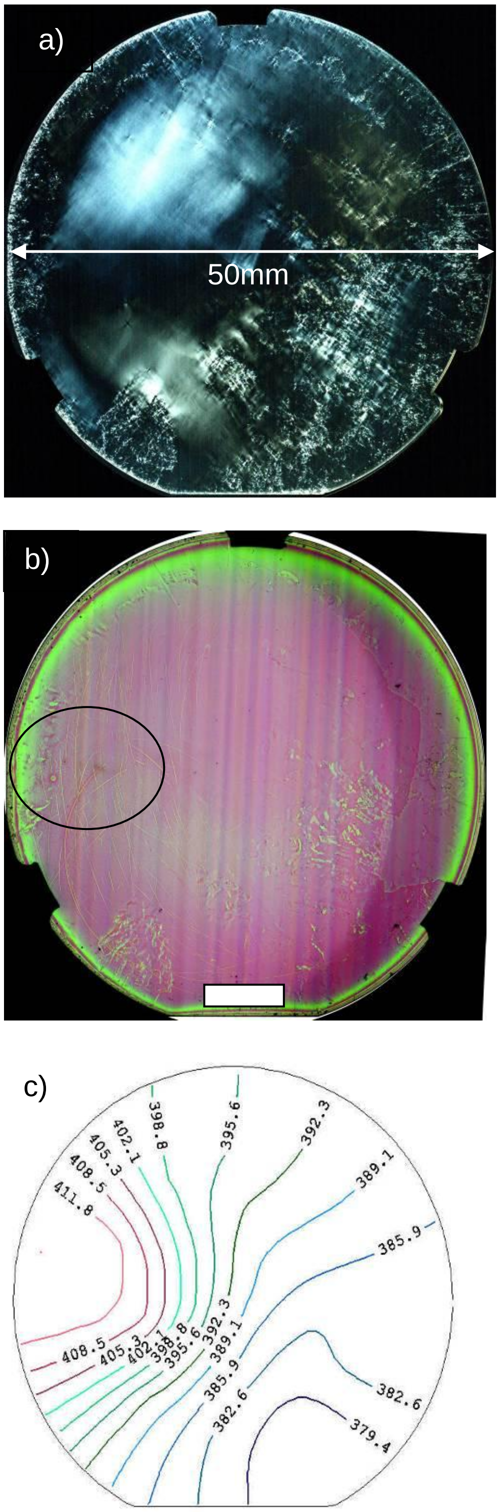

Figure 2

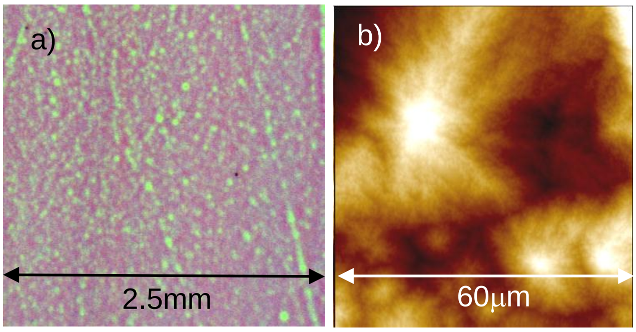

Figure 3

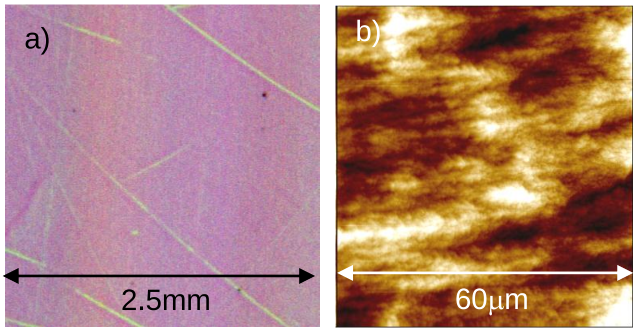

Figure 4

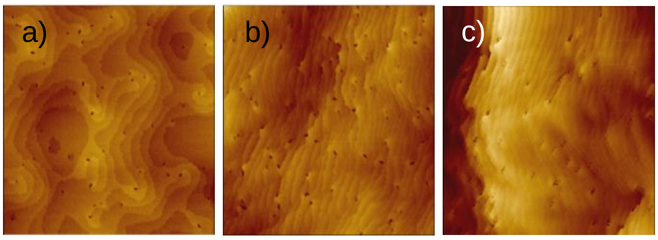

Figure 5

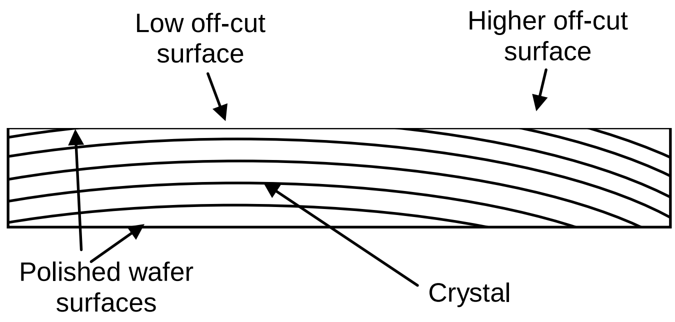
Low off-cut
surface
Higher off-cut
surface
Polished wafer
surfaces
Crystal